

Raman study of the ferroelectric semiconductor $\text{Sn}_2\text{P}_2\text{Se}_6$

P. H. M. van Loosdrecht

Research Institute of Materials, University of Nijmegen, Toernooiveld, NL-6525 ED Nijmegen, The Netherlands

M. M. Maior

*Research Institute of Materials, University of Nijmegen, Toernooiveld, NL-6525 ED Nijmegen, The Netherlands
and Institute of Physics and Chemistry of Solid State, Uzhgorod State University, 29400 Uzhgorod, Ukraine*

S. B. Molnar and Yu. M. Vysochanskii

Institute of Physics and Chemistry of Solid State, Uzhgorod State University, 29400 Uzhgorod, Ukraine

P. J. M. van Bentum and H. van Kempen

Research Institute of Materials, University of Nijmegen, Toernooiveld, NL-6525 ED Nijmegen, The Netherlands

(Received 2 February 1993)

The Raman spectrum of $\text{Sn}_2\text{P}_2\text{Se}_6$ is found to be in good agreement with the selection rules in the paraelectric and ferroelectric phases. The incommensurability has only a minor influence on the phonon scattering in $\text{Sn}_2\text{P}_2\text{Se}_6$. A broad central peak is found in the ferroelectric phase, whose intensity reaches a maximum near the lock-in phase transition. Line-shape distortions of some of the phonon modes indicate a Fano type of coupling to the excitations causing the central peak.

I. INTRODUCTION

The $\text{Sn}_2\text{P}_2\text{Se}_6$ compound is a member of the isomorphous $(\text{Pb}_x\text{Sn}_{1-x})_2\text{P}_2(\text{S}_y\text{Se}_{1-y})_6$ family of ferroelectric semiconductors. The (x, y, T) -phase diagram of this monoclinic family exhibits a ferroelectric ($x < 0.4$) and a paraelectric phase, with for $y < 0.72$ an intermediate incommensurate phase.¹ At room temperature the pure $\text{Sn}_2\text{P}_2\text{Se}_6$ compound is in a paraelectric phase with centrosymmetric space group $P2_1/c$ ($Z=2$). At $T_i=221$ K a second-order phase transition occurs to a displacively modulated incommensurate phase with the average structure of the high-temperature phase and modulation wave vector $\mathbf{q} \approx 0.075-0.085\mathbf{c}^*$. At $T_l=193$ K there is a first-order lock-in transition to a proper ferroelectric phase with space group P_c ($Z=2$).² The incommensurate phase is absent in the previously studied pure $\text{Sn}_2\text{P}_2\text{S}_6$ compound which has only a single second-order phase transition from the paraelectric to the ferroelectric phase. This phase transition is induced by the condensation of a soft mode of B_u symmetry in the high-temperature phase and of A' symmetry in the low-temperature phase.³ Due to phonon-phonon coupling the frequency of the soft mode in $\text{Sn}_2\text{P}_2\text{S}_6$ does not vanish at T_c . Apart from this phonon-phonon coupling Slivka *et al.*³ observed a coupling of the soft mode to the observed broad central peak in their Raman spectra. This is not unusual, since many ferroelectrics show a strong coupling between the phonon system and dielectric fluctuations near the ferroelectric phase transition.⁴⁻⁶ One can expect that in $\text{Sn}_2\text{P}_2\text{Se}_6$ similar coupling effects exist.

In this paper we report a Raman spectroscopic study of the dynamical properties of $\text{Sn}_2\text{P}_2\text{Se}_6$ in the paraelectric, incommensurate, and ferroelectric phases. In addition

results are reported on the temperature dependence of the low-frequency part of the Raman spectrum in the ferroelectric phase. Line-shape distortions of some of the phonons strongly indicate a Fano⁷ type of coupling to the excitations causing the broad central peak observed in the spectra.

II. EXPERIMENTAL

Nicely faceted $\text{Sn}_2\text{P}_2\text{Se}_6$ single crystals are obtained using a sublimation growth technique. The crystals used in the experiments are oriented on the basis of their morphology and by x-ray diffraction, and are mounted on the cold finger of a flow cryostat (stabilized to ± 0.1 K, absolute error ± 2 K). Polarized Raman experiments are performed in a backscattering geometry on natural crystal faces using a DILOR XY multichannel spectrometer (spectral slit width 1.5 cm^{-1}) with a Ti:Sapphire laser (740 nm, 200 mW/cm^2) as excitation source. The photon energy of the excitation used has the advantage that it is below the band-gap energy of $\text{Sn}_2\text{P}_2\text{Se}_6$, preventing excessive heating due to strong absorption as observed under 514-nm excitation.

Polarized Raman spectra ($5-2000 \text{ cm}^{-1}$) are recorded in $\mathbf{a}(\mathbf{b}, \mathbf{b})\bar{\mathbf{a}}$ and $\mathbf{a}(\mathbf{b}, \mathbf{c})\bar{\mathbf{a}}$ geometries, corresponding to $A_g(A')$ and $B_g(A'')$ symmetry in the paraelectric (ferroelectric) phase, respectively. Figure 1 shows the polarized Raman spectra recorded in the paraelectric ($T=295$ K), incommensurate ($T=210$ K), and ferroelectric phases ($T=100$ K) for $5 \text{ cm}^{-1} < \omega < 500 \text{ cm}^{-1}$. The frequencies of the peaks observed in the spectra are listed in Table I. No structure is found above 500 cm^{-1} . A large number of modes is observed at all temperatures, reflecting both the low symmetry of the crystals as well as the large num-

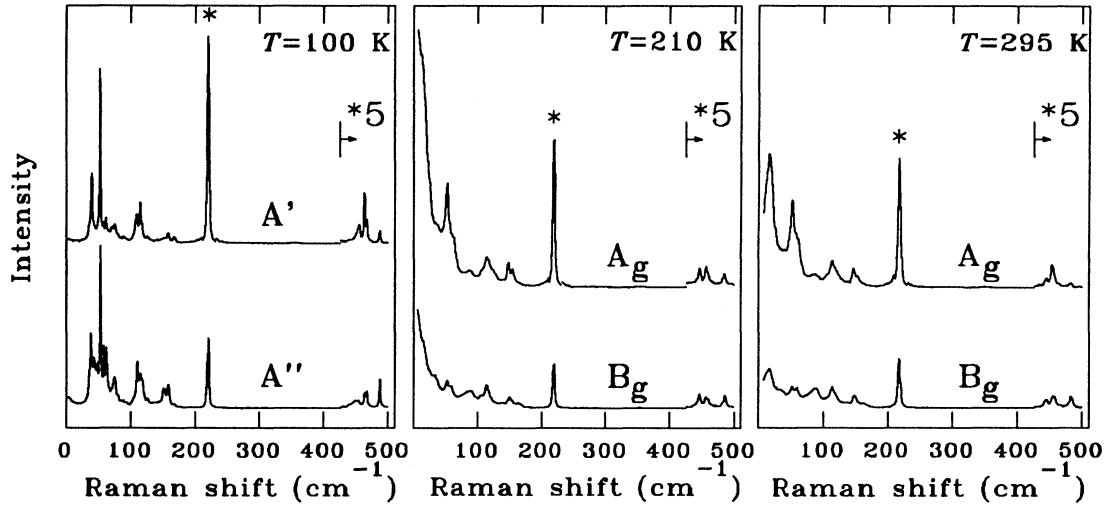


FIG. 1. Polarized Raman spectra of $\text{Sn}_2\text{P}_2\text{Se}_6$ in $\text{a}(\text{b},\text{b})\text{a}$ (A' and A_g) and $\text{a}(\text{b},\text{c})\text{a}$ (A'' and B_g) geometries for the ferroelectric ($T=100$ K), incommensurate ($T=210$ K), and paraelectric ($T=295$ K) phases. The P-P vibrations denoted by * in the $\text{a}(\text{b},\text{b})\text{a}$ spectra are scaled down by a factor of 2. Above 425 cm^{-1} the spectra are scaled up by a factor of 5.

ber of atoms (20) in the primitive cell of the structure. The total number of observed modes is given in the last row of Table I.

III. DYNAMICAL PROPERTIES OF $\text{Sn}_2\text{P}_2\text{Se}_6$

The Raman spectra of Fig. 1 show three regions of interest. The first region below 200 cm^{-1} contains the external modes and the internal Se-P-Se bending modes of the structural $(\text{PSe}_3)^{2-}$ units. Since the Se-P-Se bending modes overlap with the external modes one can ex-

pect some mixing of these modes. Therefore a distinction between external and internal modes is somewhat questionable here. The two other regions are found around 220 cm^{-1} and between 400 and 500 cm^{-1} , containing the $\text{Se}_3\text{P-PSe}_3$ and the P-Se valence vibrations, respectively.

A. Comparison of $\text{Sn}_2\text{P}_2\text{Se}_6$ to $\text{Sn}_2\text{P}_2\text{S}_6$

The frequencies of the P-P and P-S vibrational modes can be compared to the corresponding frequencies as measured in $\text{Sn}_2\text{P}_2\text{S}_6$ crystals.⁸ The $\text{S}_3\text{P-PS}_3$ vibration in

TABLE I. Peak frequencies (in cm^{-1}) of the observed modes in the polarized Raman spectra of $\text{Sn}_2\text{P}_2\text{Se}_6$ in the ferroelectric (F), incommensurate (IC), and paraelectric (P) phases, respectively. The last row gives the total number of observed modes in the spectra.

F $T=100$ K		IC $T=220$ K		P $T=295$ K		F $T=100$ K		IC $T=220$ K		P $T=295$ K	
(b,b) A'	(b,c) A''	(b,b) A_g	(b,c) B_g	(b,b) A_g	(b,c) B_g	(b,b) A'	(b,c) A''	(b,b) A_g	(b,c) B_g	(b,b) A_g	(b,c) B_g
		12	12	16	16	115	116	115	115	114	114
38	38		34		35		119				
39	43					126	126	124			
	48						141		138		
53	53	53	53	52	52	151	151	148	150	147	148
58	58		59		59	158	158	155	155	152	
62	62	63		62			168		163		162
70	70					220	220	219	219	217	217
72	73					355		351		349	
75	74						448	446	446	444	444
80	79					452	453				
85	85		83	85		454		455	455	454	453
89	88	87	87		88	463	463	460	459		457
93	93		92			467	467				
95	95					485					479
108	110	107	107			487	487	484	485	482	482
Total observed modes:						26	28	15	18	12	14

$\text{Sn}_2\text{P}_2\text{S}_6$ is found at 381 cm^{-1} . Scaling this frequency with the square root of the mass ratio $\sqrt{M_{\text{PS}_3}/M_{\text{PSe}_3}}$ yields 262 cm^{-1} . This value overestimates the measured frequency (220 cm^{-1}) in $\text{Sn}_2\text{P}_2\text{Se}_6$ by 19%. This difference originates from a difference in P-P bond strength of the anions in the two compounds mainly due to the different ion radii of the S and Se ions. From the difference between the mass scaled and observed frequencies one can estimate the P-P bond strength ratio $\lambda_{\text{Se}}/\lambda_{\text{S}}$ to be ≈ 0.70 .

In a similar manner one can compare the P-Se and P-S valence vibrations found around 470 and 575 cm^{-1} , respectively. Scaling the latter frequency with the square root of the effective masses $\mu_{\text{PS}_3, \text{PSe}_3} = 3M_{\text{P}}M_{\text{S,Se}}/(M_{\text{P}} + 3M_{\text{S,Se}})$ one finds 531 cm^{-1} , again a too high value resulting from the difference in bond strengths. The ratio between the bond strengths is estimated to be $\lambda'_{\text{Se}}/\lambda'_{\text{S}} \approx 0.78$, in good agreement with the ratio 0.82 found by Drowart *et al.*⁹ in dissociation experiments.

B. Symmetry aspects

The selection rules for inelastic light scattering are determined from a symmetry analysis of the vibrational properties of $\text{Sn}_2\text{P}_2\text{Se}_6$. For the paraelectric and ferroelectric phase this is done using a conventional factor group analysis.¹⁰ In the incommensurate phase this method is no longer appropriate. Instead, the convenient superspace approach outlined by Janssen¹¹ and Currat and Janssen¹² is used to determine the selection rules. Although in principle one should consider all modes with wave vector $\mathbf{k} = l\mathbf{q}$ ($l \in \mathbb{Z}$) only vibrational modes with $\mathbf{k} = \mathbf{0}, \pm\mathbf{q}$ are taken into account. This is justified by the absence of higher-order satellites in the x-ray-diffraction pattern.² The results of the symmetry analysis in the three phases are listed in Table II, where n_{int} , $n_{\text{trans}}^{\text{opt}}$, $n_{\text{rot}}^{\text{opt}}$, and n_{tot} correspond to the number of internal vibrational

motions of the $(\text{PSe}_3)^{2-}$ anions, external optical translational modes, external optical rotational modes, and the total number of vibrational modes of a given symmetry, respectively. The relatively low symmetry of $\text{Sn}_2\text{P}_2\text{Se}_6$ in all phases leads to a nearly equal number of active modes in the various symmetries. The selection rules found for the paraelectric and ferroelectric phases are in good agreement with the results obtained by Vysochanskii *et al.*⁸ for the isostructural $\text{Sn}_2\text{P}_2\text{S}_6$ compound.

Clearly, the spectra reveal most of the predicted modes in the paraelectric and ferroelectric phases. In the incommensurate phase more modes are observed than predicted from the selection rules for the average structure (the paraelectric phase), due to the activity of $\mathbf{k} = \pm l\mathbf{q}$ ($l \neq 0$) modes. Nevertheless, only a few additional modes are found; the total number of observed modes is much smaller than what one expects from the symmetry analysis in the incommensurate phase (see Table II). One can therefore conclude that the incommensurability has only a small influence on the dynamical properties of $\text{Sn}_2\text{P}_2\text{Se}_6$, which is a strong indication that the amplitude of the modulation is rather small.

The internal vibrations of the $(\text{PSe}_3)^{2-}$ anions (C_{3v} symmetry) can be classified as

$$\Gamma_{\text{PSe}_3^{2-}}^{C_{3v}} = 2A_1 + 2E.$$

The selection rules predict in the commensurate phases a splitting of the P-Se valence vibrations ($A_1 + E$) into six components per scattering geometry, two originating from the A_1 , and four from the doubly degenerate E mode. The multiplets found around 470 cm^{-1} indeed show 4–6 modes in each geometry. The relatively large splitting of these modes indicates a rather strong distortion of the $(\text{PSe}_3)^{2-}$ pyramids in the crystal. A similar relative splitting of these modes is found in each crystal phase indicating a nearly equal distortion in all phases, this in contrast to the situation in $\text{Sn}_2\text{P}_2\text{S}_6$ crystals.⁸

TABLE II. The number of vibrational modes at $\mathbf{k} = \mathbf{0}$ in the different phases of $\text{Sn}_2\text{P}_2\text{Se}_6$. The last column gives the activity of the modes in Raman and IR experiments. For the incommensurate phase only modes with $\mathbf{k} = \mathbf{0}$ and $\pm\mathbf{q}$ are taken into account.

Paraelectric phase ($P2_1/c$)					
irrep.	n_{int}	$n_{\text{trans}}^{\text{opt}}$	$n_{\text{rot}}^{\text{opt}}$	n_{tot}	activity
A_g	6	6	3	15	(a,a),(b,b),(c,c),(a,c)
B_g	6	6	3	15	(a,b),(b,c)
A_u	6	5	3	14	b
B_u	6	4	3	13	a, c
Incommensurate phase ($P2_1/c$, $q \approx 0.08c^*$, $l = 0, \pm 1$)					
irrep.	n_{int}	$n_{\text{trans}}^{\text{opt}}$	$n_{\text{rot}}^{\text{opt}}$	n_{tot}	activity
A_g	12	12	6	30	(a,a),(b,b),(c,c),(a,c)
B_g	12	12	6	30	(a,b),(b,c)
A_u	12	11	6	29	b
B_u	12	10	6	28	a, c
Ferroelectric phase (P_c)					
irrep.	n_{int}	$n_{\text{trans}}^{\text{opt}}$	$n_{\text{rot}}^{\text{opt}}$	n_{tot}	activity
A'	12	10	6	28	a,c;(a,a),(b,b),(c,c),(a,c)
A''	12	11	6	29	b;(a,b),(b,c)

The two $(\text{P}_2\text{Se}_6)^{4-}$ units per primitive cell lead to two P-P vibrations at $\mathbf{k}=\mathbf{0}$ which correspond to in-phase (A' or A_g symmetry) and out-of-phase (A'' or B_g) vibrations of the two P-P bonds, respectively. One can expect that the out-of-phase vibration has a smaller second-order polarizability than in the in-phase vibration. This is indeed observed in the difference of the intensities of the P-P peak in the A' (A_g) and A'' (B_g) spectra.

IV. LOW-ENERGY SCATTERING

Slivka *et al.*³ have measured the temperature dependence of the soft mode at 32 cm^{-1} in $\text{Sn}_2\text{P}_2\text{S}_6$ associated with the ferroelectric phase transition, revealing a strong coupling of this mode with a Raman-active lattice mode at 40 cm^{-1} . In addition, they proposed a coupling of the soft mode to the observed "central peak" in their spectra. Figure 2(a) shows the low-frequency $c(\mathbf{a},\mathbf{a})\bar{c}$ Raman spectrum of $\text{Sn}_2\text{P}_2\text{Se}_6$ at various temperatures. Also in this case low-frequency scattering reminiscent of a central peak is observed, with an intensity increasing with temperature to a maximum at or slightly above the ferroelectric-incommensurate phase transition. At temperatures far above the incommensurate-paraelectric phase transition the quasielastic scattering has strongly decreased. In the incommensurate phase a new mode appears in the spectrum at 12 cm^{-1} . This mode hardens with temperature and at room temperature it is found at 16 cm^{-1} .

The temperature dependence of the frequencies plotted in Fig. 2(b) shows a softening of three of the modes at 38, 53, and 61 cm^{-1} . In particular the frequencies of the modes at 38 and 53 cm^{-1} decrease strongly upon approaching the phase transition at $T=293\text{ K}$. None of these modes show the usual $\omega \approx (T_0 - T)^\gamma$ behavior of an uncoupled soft mode near the phase transition. The temperature dependence of the frequencies and intensities give no direct evidence for phonon-phonon interactions, however. Instead a deformation of the line shape is observed for the modes at 38 and 53 cm^{-1} . The form of the line-shape distortion strongly indicates a coherent cou-

pling of these phonons to a continuum of excitations in the crystal, i.e., a Fano-type coupling.⁷ The origin of the continuum of states, i.e., of the observed quasielastic scattering and line-shape distortions is at present unknown. A good candidate for these states, however, is the continuum arising from the dynamics of the local dipole moments in the ferroelectric phase of $\text{Sn}_2\text{P}_2\text{Se}_6$. Another possibility is that the low-energy scattering is due to the electronic excitations in this semiconducting material. The spectral intensity of such a coupled system can be described as^{7,13}

$$I(\epsilon) \propto \frac{\epsilon + q}{(1 + \epsilon^2)}, \quad (1)$$

with $\epsilon = 2(\omega - \omega_0)/\Gamma$, ω_0 the perturbed phonon frequency, and q the so-called Fano parameter which is in first order inversely proportional to the interaction strength (V) and the density of continuum states (ρ). The linewidth Γ is proportional to ρV^2 . Figure 3(a) shows the results of a fit of Eq. (1) to the experimental line shape of the 38-cm^{-1} mode for several temperatures in the ferroelectric phase. In these fits the incoherent part of the continuum scattering is taken to decrease linearly upon increasing Raman shift. A good fit is obtained for all temperatures in the range 20–185 K. Only very close to the phase transition the fit breaks down, mainly due to the weak phonon part in the spectra. The perturbed phonon frequency is found to be $\omega_0 = 37.5 \pm 0.2\text{ cm}^{-1}$ for all curves. The resulting fit parameters q^{-1} and Γ are shown in Fig. 3(b). Above 130 K, up to close to the lock-in phase transition both q^{-1} and Γ increase approximately linearly with temperature. This indicates that the interaction strength V does not vary strongly with temperature, and that the temperature dependence of both q^{-1} and Γ is caused by an increasing density of continuum states towards the phase transition. A more direct measure for the density of continuum states is the intensity of the scattered light well below the phonon resonance, which is indeed found to be increasing more or less linearly with increasing temperature for $130\text{ K} < T < 190\text{ K}$.

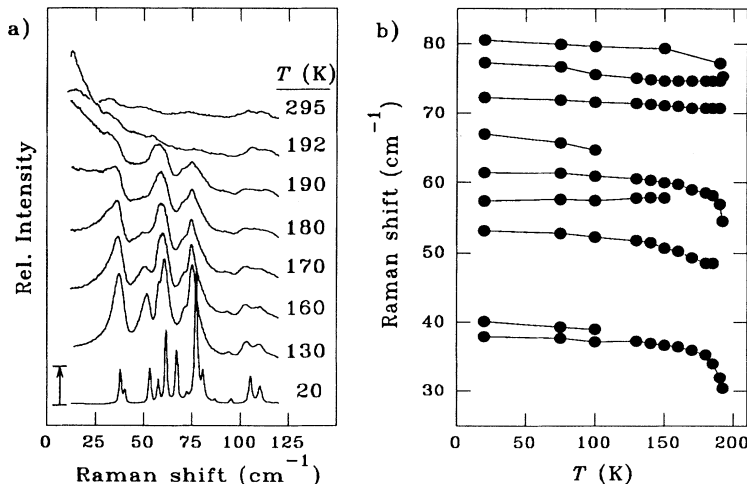


FIG. 2. (a) Temperature dependence of the low-frequency part of the $(\mathbf{a},\mathbf{a})\bar{c}$ Raman spectrum of $\text{Sn}_2\text{P}_2\text{Se}_6$ in the ferroelectric phase. The intensities are relative to the integrated intensity of the P-P vibration at 220 cm^{-1} . For clarity each subsequent curve has been given an offset indicated by the arrow in the lower left corner. (b) Temperature dependence of the peak frequency of the low-frequency energy in the $(\mathbf{a},\mathbf{a})\bar{c}$ spectrum of $\text{Sn}_2\text{P}_2\text{Se}_6$ in the ferroelectric phase.

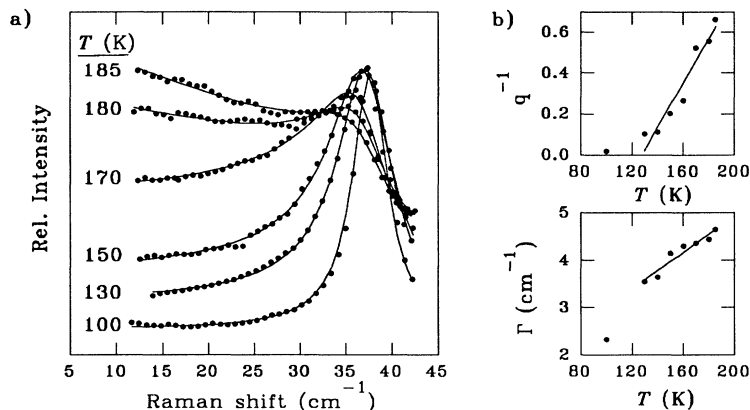


FIG. 3. (a) Fit of the Fano profile [Eq. (1)] superimposed on a linear underground to the 38 cm^{-1} Raman peak at various temperatures in the ferroelectric phase. (b) The resulting parameters q^{-1} (upper part) and Γ (lower part) of the fits shown in (a) as a function of the temperature. The solid lines are a guide to the eye.

V. CONCLUSIONS

The number of modes observed in the polarized Raman spectra recorded in the ferroelectric and paraelectric phases are in good agreement with the selection rules. In the incommensurate phase, however, the number of observed phonon modes is far less than the number of active modes predicted by the selection rules, despite the fact that only modes with $\mathbf{k}=\mathbf{0}, \pm\mathbf{q}$ have been taken into account.

At low frequencies a strong central peak is observed in the ferroelectric phase, which reaches a maximum intensity at or above the lock-in phase transition. The coupling of this low-energy scattering to the phonons lead to a Fano type of distortion of the phonon peak. The temperature dependence of the linewidth and Fano parameter in the ferroelectric phase indicates an increasing density of continuum states upon approaching the lock-in phase transition. While the precise origin of the low-energy scattering remains unknown at present, the fluctuations causing it are strongly related to the ferroelectric-incommensurate phase transition. It may very well be that the fluctuations are indeed due to the dynamics of the domain walls in the ferroelectric phase which remain as discommensurations or solitons in the incommensurate phase, consistent with the persistence of the quasielastic scattering in the incommensurate phase.

ACKNOWLEDGMENTS

We are grateful to M. I. Gurzan for providing the crystals. One of us (M.M.M.) would like to express his thanks to the staff of the Research Institute of Materials of the University of Nijmegen for their hospitality and assistance, and the Dutch and former Soviet Union governments for financial support through a cultural exchange program. Part of this work was financially supported by the Dutch Foundation for Fundamental Research of Matter (FOM).

- ¹Yu. M. Vysochanskii, M. M. Maior, V. M. Rizak, V. Yu. Slivka, and M. M. Khoma, *Zh. Eksp. Teor. Fiz.* **95**, 1355 (1989) [*Sov. Phys. JETP* **68**, 782 (1989)].
- ²T. K. Barsamian, S. S. Khasanov, V. Sh. Shekhtman, Yu. M. Vysochanskii, and V. Yu. Slivka, *Ferroelectrics* **67**, 47 (1986).
- ³V. Yu. Slivka, Yu. M. Vysochanskii, M. I. Gurzan, and D. V. Chepur, *Fiz. Tverd. Tela (Leningrad)* **20**, 3530 (1978) [*Sov. Phys. Solid State* **20**, 2042 (1978)].
- ⁴G. Harbeke, E. F. Steigemeier, and R. K. Wehner, *Solid State Commun.* **8**, 1765 (1970).
- ⁵J. F. Scott, *Rev. Mod. Phys.* **46**, 83 (1974).
- ⁶R. A. Cowley and G. J. Coombs, *J. Phys. C* **6**, 143 (1973).
- ⁷U. Fano, *Phys. Rev.* **124**, 1866 (1961).
- ⁸Yu. M. Vysochanskii, V. Yu. Slivka, Yu. V. Voroshilov, M. I.

- Gurzan, and D. V. Chepur, *Fiz. Tverd. Tela (Leningrad)* **21**, 211 (1979) [*Sov. Phys. Solid State* **21**, 123 (1979)].
- ⁹J. Drowart, C. E. Myers, R. Szwarc, E. van der Ausera-Mahieu, and O. M. Uy, *High Temp. Sci.* **5**, 482 (1973).
- ¹⁰See, for instance, G. Turrel, *Infrared and Raman Spectra of Crystals* (Academic, London, 1972).
- ¹¹T. Janssen, *J. Phys. C* **12**, 5381 (1979).
- ¹²R. Currat and T. Janssen, in *Solid State Physics: Advances in Research & Applications*, edited by H. Ehrenreich (Academic, New York, 1988), Vol. 41, p. 210.
- ¹³M. V. Klein, *Light Scattering in Solids I*, Topics in Applied Physics Vol. 8, edited by M. Cardona (Springer-Verlag, Berlin, 1983), p. 169.